SUPPLEMENTARY FIGURE LEGENDS

Figure S1. CSB promotes recruitment of the BRCA1-C complex to DSBs. (**A**) Representative images of U2OS-265 WT and CSB-KO cells with induction of FokI expression. Fixed cells were costained with anti-CSB and anti-γH2AX antibodies. Nuclei were stained with DAPI in blue in this and following figures. Scale bars in this and subsequent figures: 5 μm. (**B**) Quantification of the intensity of CSB signal at the site of FokI-induced DSBs in U2OS-265 WT and CSB KO cells from (A). γH2AX staining was used to mark the FokI-induced damage site. Cells positive for γH2AX were used for analysis of CSB signal intensity. The respective numbers of cells analyzed for WT and CSB KO cells were 103 and 132. Data are represented as a scatter plot graph with the mean indicated. The *P* value was determined using non-parametric Mann-Whitney rank-sum *t*-test. (**C**) Representative IF images of U2OS-265 CSB-KO cells with induction of FokI expression. Fixed cells were stained with an anti-γH2AX antibody in conjunction with antibodies against various endogenous proteins as indicated. (**D**) Quantification of the average intensity of MRE11 signal at the site of FokI-induced DSBs in U2OS-265 WT and CSB KO cells. Standard deviations from three independent experiments are indicated. The *P* value was determined using a Student's two-tailed unpaired t test. (**E**) Quantification of cells with ≥ 10 IR-induced MRE11 foci. hTERT-RPE WT and CSB-KO cells were treated with 2 Gy IR and fixed 1 h later. Standard deviations from three indepenent experiments are indicated. (**F**) Quantification of cells with ≥ 10 IR-induced NBS1 foci. hTERT-RPE WT and CSB-KO cells were treated with 2 Gy IR and fixed 1 h later. Standard deviations from three indepenent experiments are indicated.

Figure S2. CSB colocalizes with the BRCA1-C complex at the lac operator array. (**A**) Representative images of U2OS-265 CSB-KO cells expressing the vector alone or mCherry-LacR-CSB. Cells were fixed and stained with antibodies against various proteins as indicated. (**B**) Quantification of vector- and mCherry-LacR-CSB-expressing U2OS-265 CSB-KO cells exhibiting RAP80 accumulation at the lac

operator array. At least 100 cells positive for mCherry staining were scored per condition in a blind manner. Standard deviations from three independent experiments are indicated. (**C**) Quantification of vector-, mCherry-LacR-CSB, mCherry-LacR-CSB-W851R and mCherry-LacR-CSB-ΔN30-expressing U2OS-265 CSB-KO cells exhibiting BRCA1 accumulation at the lac operator array. Scoring was done as in S2B. Standard deviations from three independent experiments are indicated.

Figure S3. Knockdown of BRCA1 does not affect the interaction of CSB with MRN and vice versa. (**A**) Representative images of mCherry-LacR-CSB-expressing U2OS-265-CSB-KO cells transfected with various siRNAs as indicated. Fixed cells were stained with an anti-BRCA1 antibody. (**B**) Representative images of mCherry-LacR-CSB-expressing U2OS-265-CSB-KO cells transfected with various siRNAs as indicated. Fixed cells were stained with an anti-NBS1 antibody. (**C**) Representative images of mCherry-LacR-CSB-expressing U2OS-265-CSB-KO cells transfected with various siRNAs as indicated. Fixed cells were stained with an anti-CtIP antibody. (**D**) Representative images of mCherry-LacR-CSB-expressing U2OS-265-CSB-KO cells transfected with various siRNAs as indicated. Fixed cells were stained with an anti-MRE11 antibody.

Figure S4. CSB interacts with MRN and BRCA1 through two distinct regions, with the former requiring the WHD. (**A**) Representative images of U2OS-265-CSB-KO cells expressing mCherry-LacR-MRE11 in conjunction with various Myc-CSB alleles as indicated. (**B &C**) Representative images of U2OS-265-CSB-KO cells expressing mCherry-LacR-BRCA1 in conjunction with various Myc-CSB alleles as indicated.

Figure S5. CSB phosphorylation on S1276 mediates its interaction with the BRCT domain of BRCA1. (**A**) Representative images of U2OS-265-CSB-KO cells expressing mCherry-LacR-CSB in conjunction with various GFP-BRCA1 alleles as indicated. (**B**) Representative images of U2OS-265-CSB-KO cells

expressing mCherry-LacR-CSB in conjunction with various Flag-BRCA1 alleles as indicated. (**C**) Quantification of percentage of cells with various Flag-BRCA1 alleles at the lac operator array. At least 250 cells positive for expression of Flag-tagged BRCA1 alleles were scored per condition in a blind manner. Standard deviations from three independent experiments are indicated. (**D**) Representative images of U2OS-265-CSB-KO cells expressing various mCherry-LacR-CSB alleles as indicated. (**E**) Representative images of U2OS-265-CSB-KO cells expressing GFP-BRCA1-BRCT in conjunction with various mCherry-LacR-CSB alleles as indicated.

Figure S6. CSB phosphorylation on S1276 promotes efficient recruitment of the BRCA1-C complex to FokI-induced DSBs. (**A-D**) Representative images of U2OS-265 CSB-KO cells with induction of FokI expression. Fixed cells were stained with anti-γH2AX antibody in conjunction with anti-BRCA1 (A), anti-MRE11 (B), anti-CtIP (C) or anti-RIF1 (D).

Figure S7. Loss of CSB does not affect AsiSI-induced cleavage. (**A**) Schematic diagram of AsiSI-induced DSB1 and DSB 2 on chromosome 1. The position of three different pairs of primers flanking DSB1 and DSB2 are indicated. (**B**) Western analysis of AID-DIvA-U2OS WT, CSB-KO-1 and CSB-KO-2. Immunoblotting was done with anti-CSB and anti-γ-tubulin antibodies. (**C**) Quantification of DNA cleavage at AsiSI-induced DSB1 on chromosome 1 in AID-DIvA-U2OS WT, CSB-KO clone 1 (KO-1) and CSB-KO clone 2 (KO-2). Standard deviations from three independent experiments are indicated. (**D**) Quantification of DNA cleavage at AsiSI-induced DSB2 on chromosome 1 in AID-DIvA-U2OS WT, CSB-KO clone 1 (KO-1) and CSB-KO clone 2 (KO-2). Standard deviations from three independent experiments are indicated.

Figure S8. Loss of CSB impairs the amount of ssDNA generated from DSBs. (**A**) Quantification of the amount of ssDNA. AID-DIvA-U2OS WT, CSB-KO-1 and CSB-KO-2 were treated with no 4-OHT or 4-

OHT for 1 h , 2 h or 4 h. The amount of ssDNA generated at three different positions 335 nt, 1618 nt or 3500 nt from of AsiSI-induced DSB1 was measured as described in “Methods”. Standard deviations from three indepenent experiments are indicated. **P*<0.05; ***P*<0.01; ****P*<0.001. n.s., *P*>0.05. (**B**) Quantification of the amount of ssDNA. AID-DIvA-U2OS WT, CSB-KO-1 and CSB-KO-2 were treated with no 4-OHT or 4-OHT for 1 h , 2 h or 4 h. The amount of ssDNA generated at three different positions 364 nt, 1754 nt or 3564 nt from of AsiSI-induced DSB2 was measured as described in “Methods”. Standard deviations from three indepenent experiments are indicated. **P*<0.05; ***P*<0.01; ****P*<0.001. (**C**) Quantification of the amount of ssDNA. AID-DIvA-U2OS WT, CSB-KO-1 and CSB-KO-2 were treated with no 4-OHT or 4-OHT for 1 h , 2 h or 4 h. The amount of ssDNA generated at a location containing no AsiSI restriction site on chromosome 22 was measured as described in “Methods”. Standard deviations from three indepenent experiments are indicated.

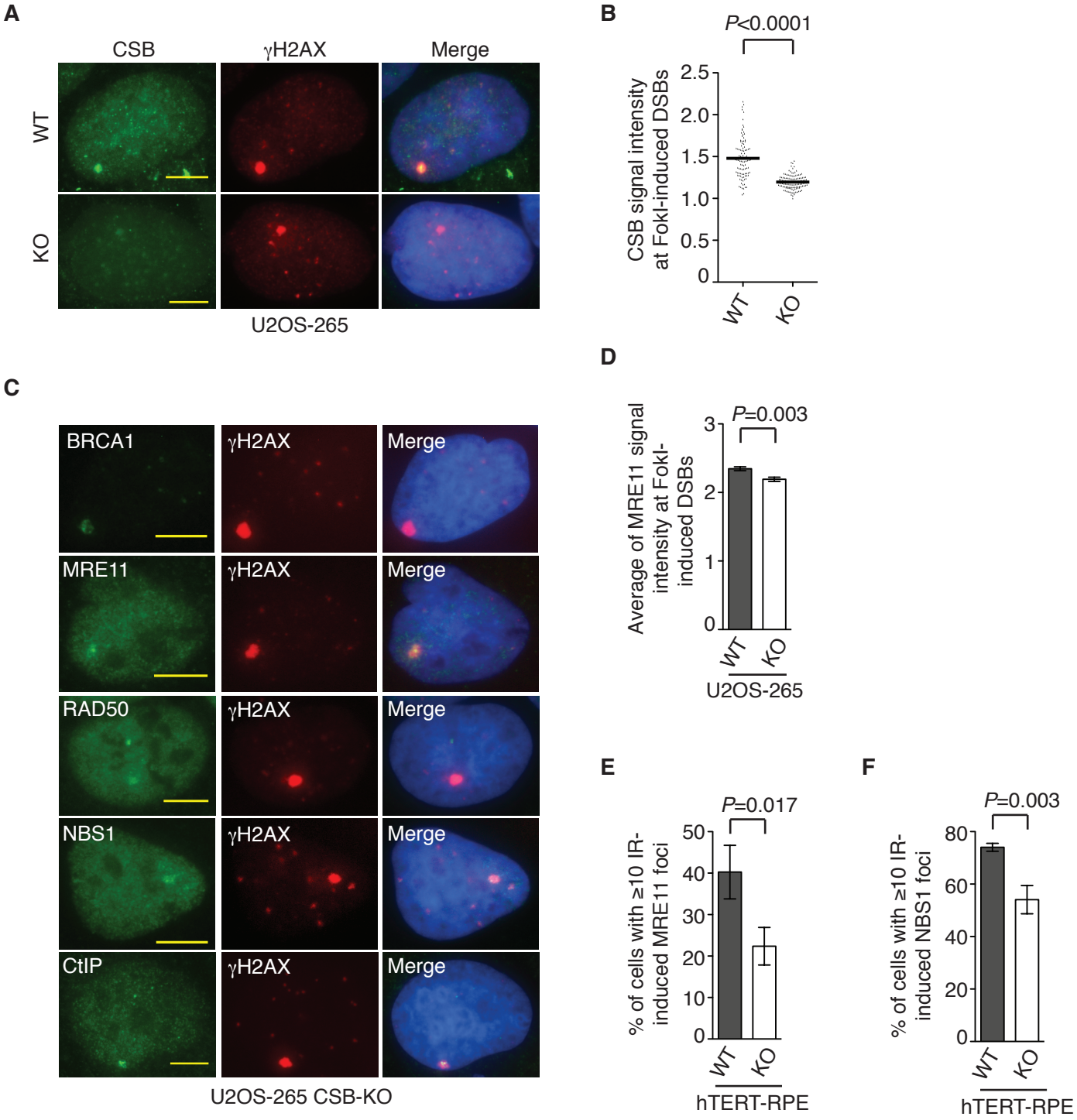
A
CSB
γH2AX
Merge
WT
KO
U2OS-265
B
P<0.0001
CSB signal intensity at FokI-induced DSBs
2.5
2.0
1.5
1.0
0.5
0
WT
KO
C
BRCA1
MRE11
RAD50
NBS1
CtIP
γH2AX
Merge
U2OS-265 CSB-KO
D
P=0.003
Average of MRE11 signal intensity at FokI-induced DSBs
3
2
1
0
WT
KO
U2OS-265
E
P=0.017
% of cells with ≥10 IR-induced MRE11 foci
50
40
30
20
10
0
WT
KO
hTERT-RPE
F
P=0.003
% of cells with ≥10 IR-induced NBS1 foci
80
60
40
20
0
WT
KO
hTERT-RPE

A

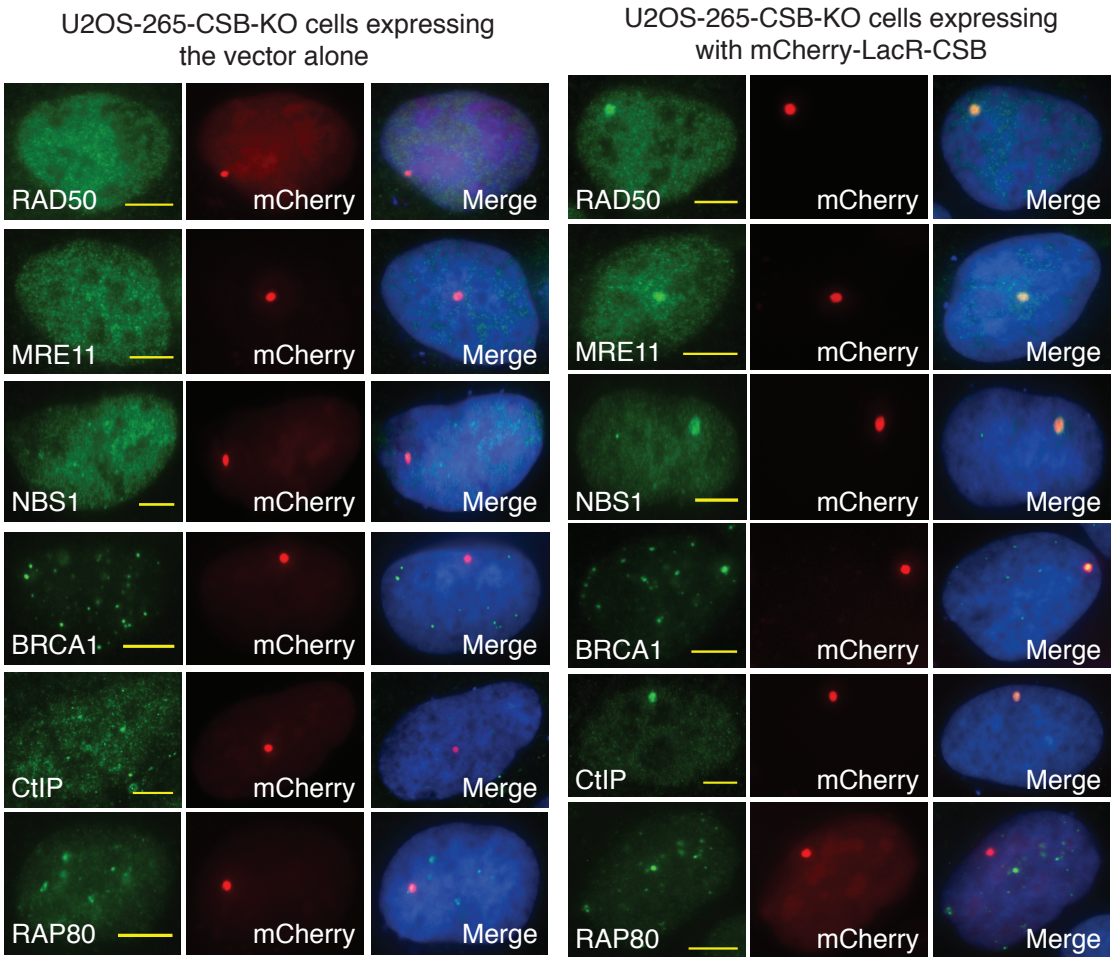
U2OS-265-CSB-KO cells expressing the vector alone
U2OS-265-CSB-KO cells expressing with mCherry-LacR-CSB
RAD50
mCherry
Merge
MRE11
NBS1
BRCA1
CtIP
RAP80

B

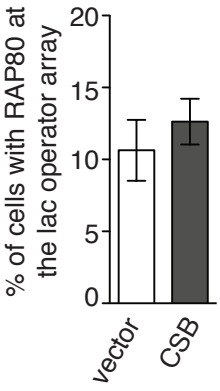
% of cells with RAP80 at the lac operator array
0
5
10
15
20
vector
CSB

C

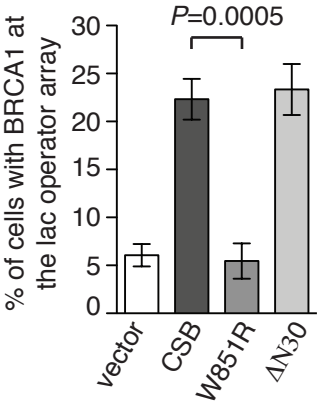
% of cells with BRCA1 at the lac operator array
P=0.0005
0
5
10
15
20
25
30
vector
CSB
W851R
ΔN30

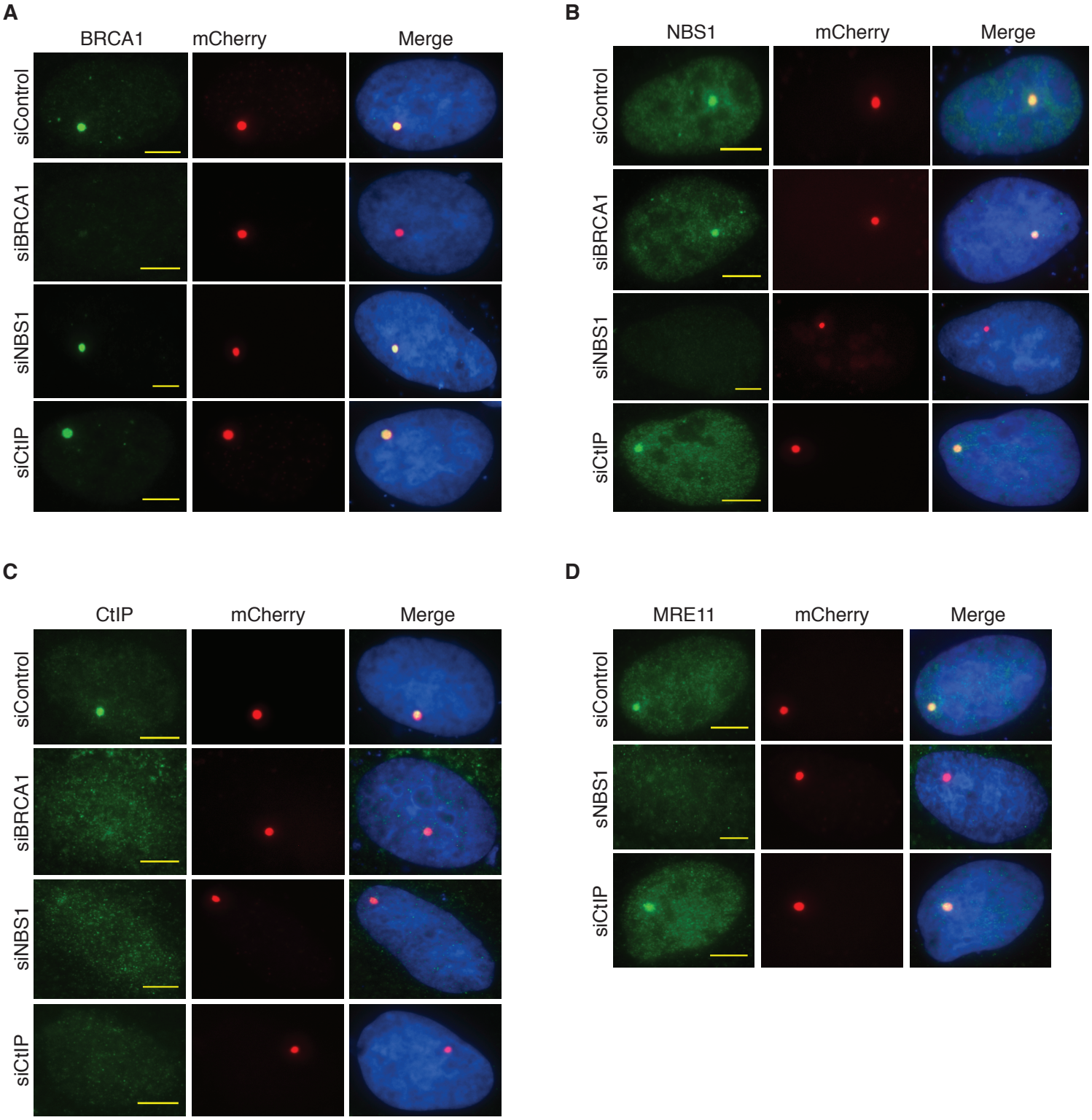
A
BRCA1
mCherry
Merge
siControl
siBRCA1
siNBS1
siCtIP
B
NBS1
mCherry
Merge
siControl
siBRCA1
siNBS1
siCtIP
C
CtIP
mCherry
Merge
siControl
siBRCA1
siNBS1
siCtIP
D
MRE11
mCherry
Merge
siControl
sNBS1
siCtIP

A

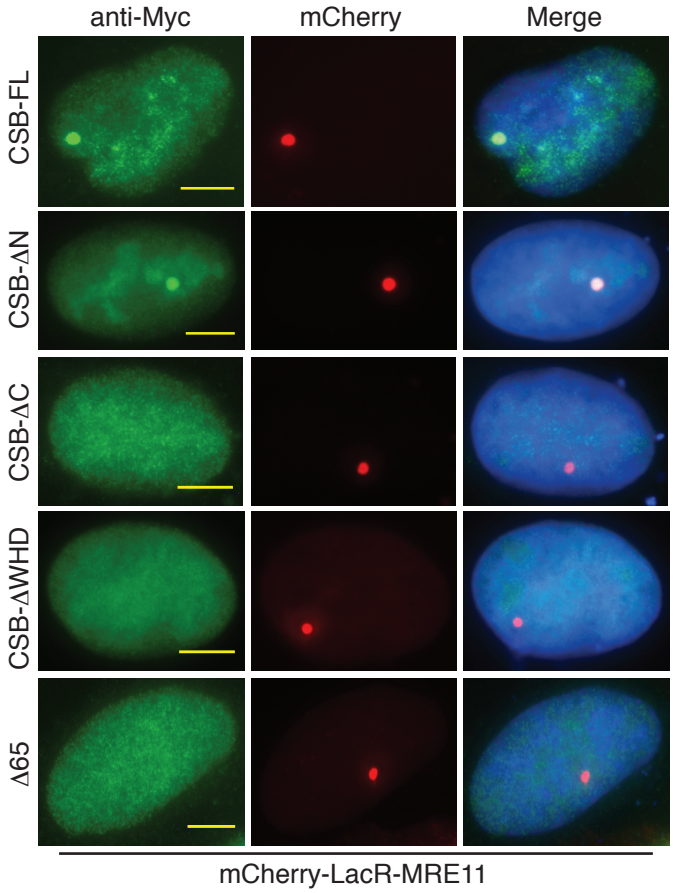
anti-Myc
mCherry
Merge
CSB-FL
CSB-ΔN
CSB-ΔC
CSB-ΔWHD
Δ65
mCherry-LacR-MRE11

B

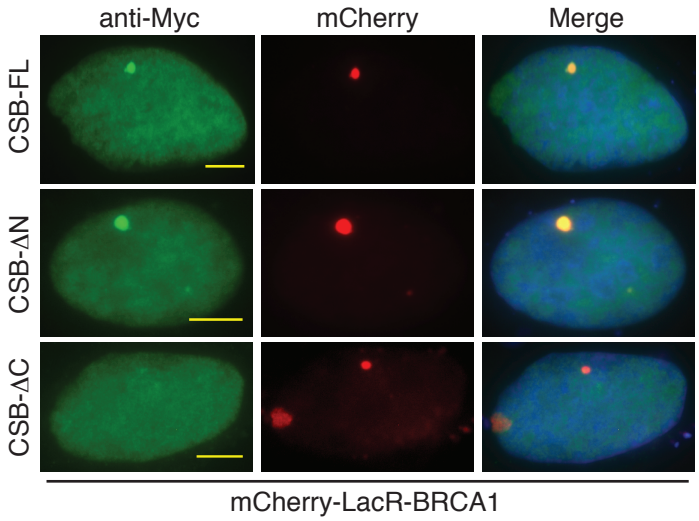
anti-Myc
mCherry
Merge
CSB-FL
CSB-ΔN
CSB-ΔC
mCherry-LacR-BRCA1

C

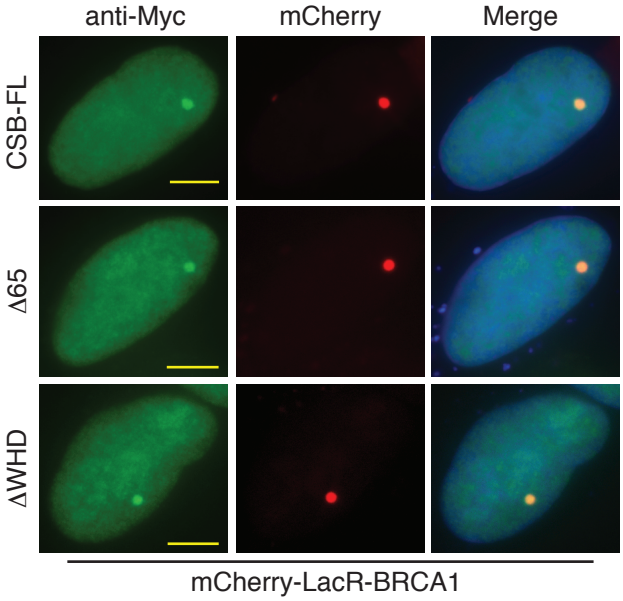
anti-Myc
mCherry
Merge
CSB-FL
Δ65
ΔWHD
mCherry-LacR-BRCA1

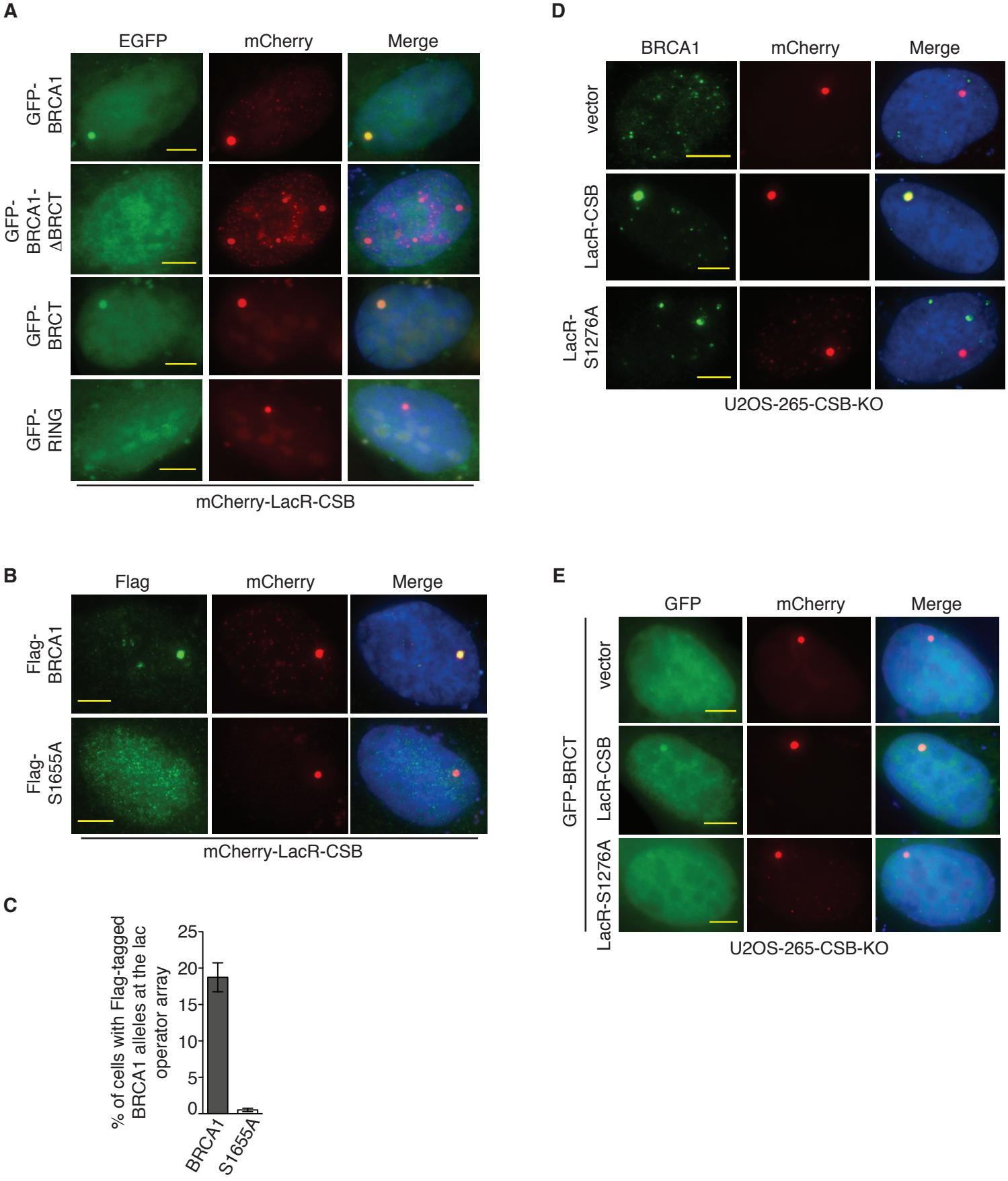
A
EGFP
mCherry
Merge
GFP-BRCA1
GFP-BRCA1-ΔBRCT
GFP-BRCT
GFP-RING
mCherry-LacR-CSB
B
Flag
mCherry
Merge
Flag-BRCA1
Flag-S1655A
mCherry-LacR-CSB
C
% of cells with Flag-tagged BRCA1 alleles at the lac operator array
25
20
15
10
5
0
BRCA1
S1655A
D
BRCA1
mCherry
Merge
vector
LacR-CSB
LacR-S1276A
U2OS-265-CSB-KO
E
GFP
mCherry
Merge
GFP-BRCT
vector
LacR-CSB
LacR-S1276A
U2OS-265-CSB-KO

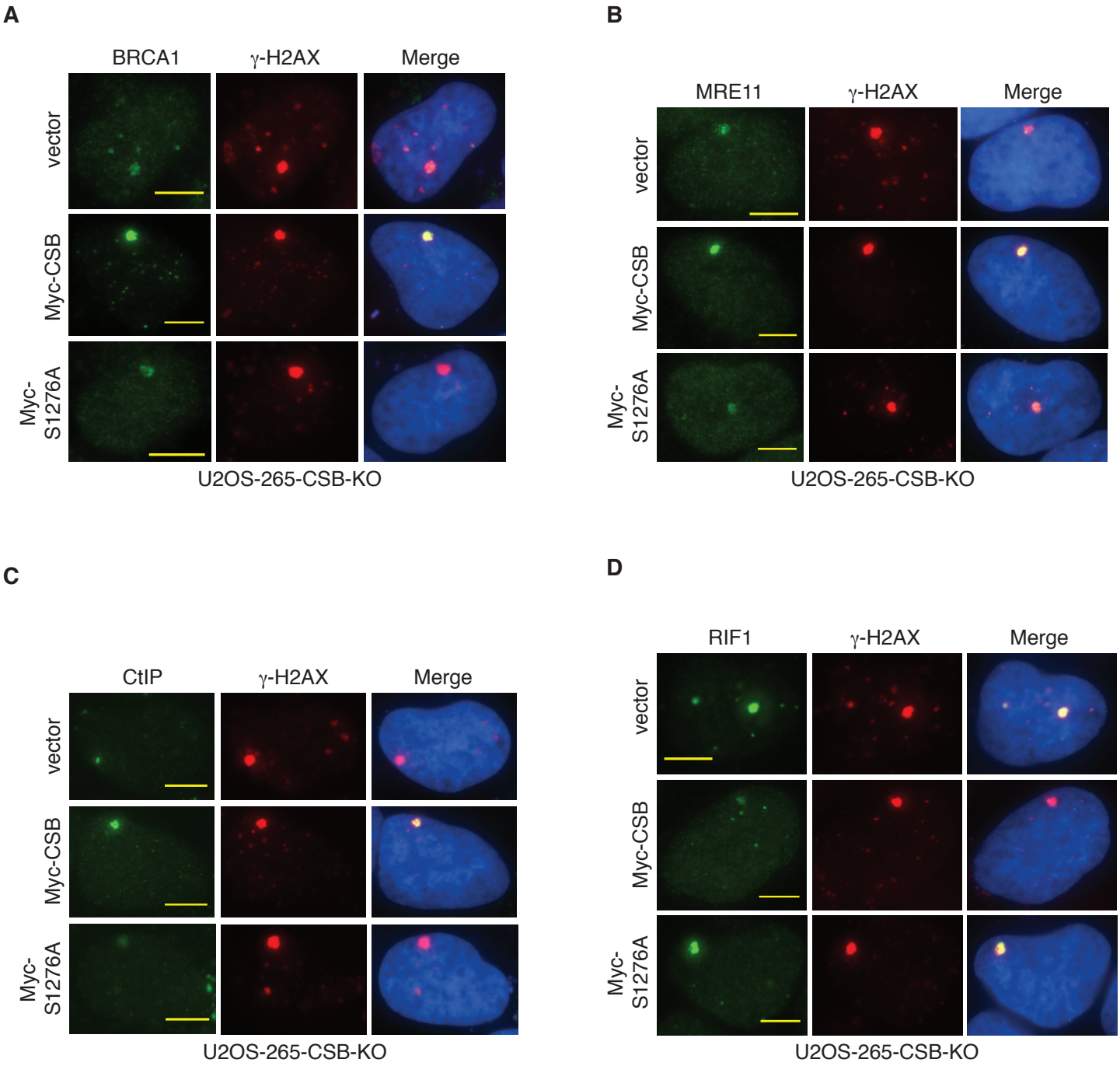
A
BRCA1
γ-H2AX
Merge
vector
Myc-CSB
Myc-S1276A
U2OS-265-CSB-KO
B
MRE11
γ-H2AX
Merge
vector
Myc-CSB
Myc-S1276A
U2OS-265-CSB-KO
C
CtIP
γ-H2AX
Merge
vector
Myc-CSB
Myc-S1276A
U2OS-265-CSB-KO
D
RIF1
γ-H2AX
Merge
vector
Myc-CSB
Myc-S1276A
U2OS-265-CSB-KO

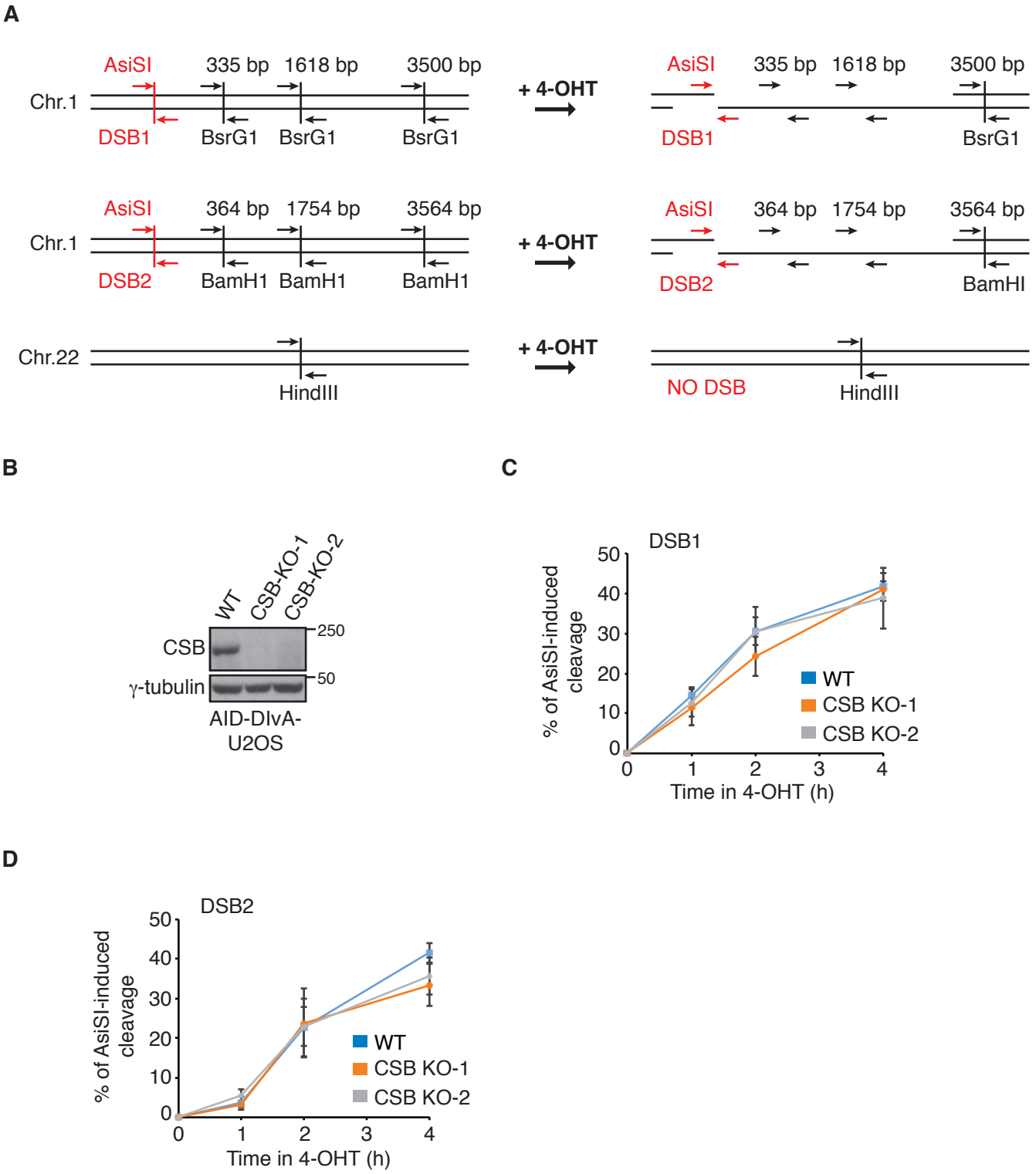
A
AsiSI
335 bp
1618 bp
3500 bp
Chr.1
DSB1
BsrG1
BsrG1
BsrG1
+ 4-OHT
AsiSI
335 bp
1618 bp
3500 bp
DSB1
BsrG1
AsiSI
364 bp
1754 bp
3564 bp
Chr.1
DSB2
BamH1
BamH1
BamH1
+ 4-OHT
AsiSI
364 bp
1754 bp
3564 bp
DSB2
BamHI
Chr.22
HindIII
+ 4-OHT
NO DSB
HindIII
B
WT
CSB-KO-1
CSB-KO-2
CSB
γ-tubulin
250
50
AID-DIvA-
U2OS
C
DSB1
% of AsiSI-induced cleavage
50
40
30
20
10
0
0
1
2
3
4
Time in 4-OHT (h)
WT
CSB KO-1
CSB KO-2
D
DSB2
% of AsiSI-induced cleavage
50
40
30
20
10
0
0
1
2
3
4
Time in 4-OHT (h)
WT
CSB KO-1
CSB KO-2

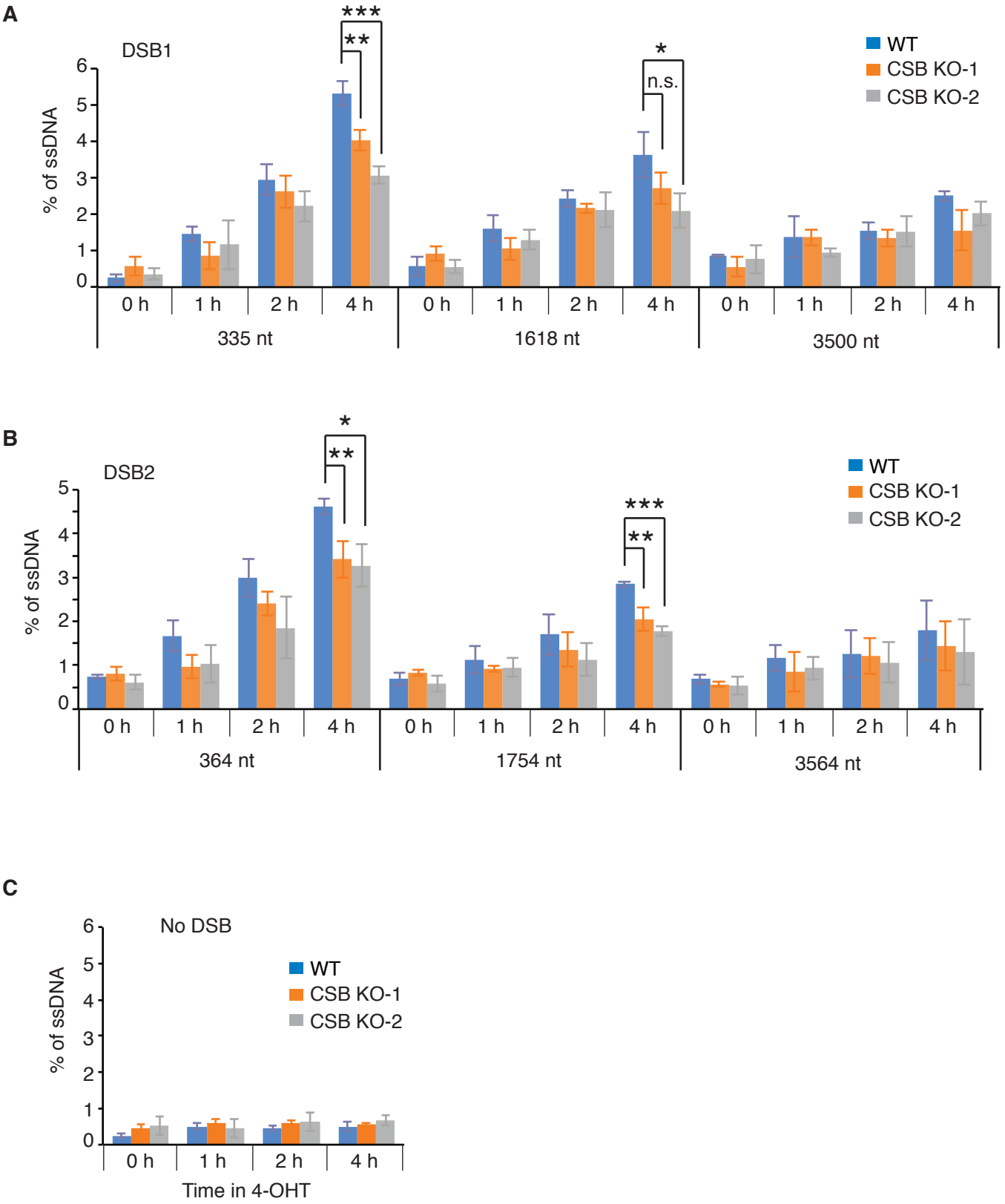
A
DSB1
% of ssDNA
0
1
2
3
4
5
6
***
**
*
n.s.
WT
CSB KO-1
CSB KO-2
0 h
1 h
2 h
4 h
335 nt
1618 nt
3500 nt
B
DSB2
% of ssDNA
0
1
2
3
4
5
*
**
***
**
WT
CSB KO-1
CSB KO-2
0 h
1 h
2 h
4 h
364 nt
1754 nt
3564 nt
C
No DSB
% of ssDNA
0
1
2
3
4
5
6
WT
CSB KO-1
CSB KO-2
0 h
1 h
2 h
4 h
Time in 4-OHT